Journal of the Korean Nuclear Society
Volume 28, Number 3, pp. 229~246, June 1996

Development of a Mechanistic Fission Gas Release Model for LWR UO_2 Fuel Under Steady-State Conditions

Yang-Hyun Koo and Dong-Seong Sohn
Korea Atomic Energy Research Institute
P.O.Box 105, Yusong, Taejon 305-500, Korea

(Received October 27, 1994)

Abstract

A mechanistic model has been developed to predict the release behavior of fission gas during steady-state irradiation of LWR UO_2 fuel. Under the assumption that UO_2 grain surface is composed of fourteen identical circular faces and grain edge bubble can be represented by a triangulated tube around the circumference of three circular grain faces, it introduces the concept of continuous formation of open grain edges tunnels that is proportional to grain edge swelling. In addition, it takes into account the interaction between the gas release from matrix to grain boundary and the reintroduction of gas atoms into the matrix by the irradiation-induced re-solution of grain face bubbles. It also treats analytically the behavior of intragranular, intergranular, and grain edge bubbles under the assumption that both intragranular and intergranular bubbles are uniform in both radius and number density. Comparison of the present model with experimental data shows that the model's prediction produces reasonable agreement for fuel with centerline temperatures of 1000 to 1400°C, wide scatter band for fuel with centerline temperatures lower than 1000°C, and underprediction for fuel with centerline temperatures higher than 1400°C.

1. Introduction

The thermal and mechanical design of fuel requires that fission gas production and release from the fuel be known accurately throughout the lifetime of the fuel. This information is needed to calculate the buildup of internal pressure of fuel and the reduction of thermal conductivity of the filling gases during irradiation. It is therefore apparent that fission gas release from fuel pellets during operation is of considerable importance in assessing the behavior of nuclear fuels.

Up to the present, a great number of fission gas models had been developed and some of them were reviewed in detail by Villalobos et al. [1] based on the approaches they had taken. Since it is generally difficult that even the most sophisticated model can consider all the pertinent processes simultaneously, each model has some shortcomings over the other models in some respects as well as some advantages in other respects.

Inspection of the literature reveals that following two points need to be improved further. The first one is that interaction between the con- centration of gas atoms in matrix and that at grain face were treated rather simply under irradiation conditions. As more fission gas atoms are produced in the matrix and more fission gas atoms are accumulated in both

intragranular and intergranular bubbles, the phenomenon of re-solution of the gas atoms from both intragranular and intergranular bubbles becomes more important since the amount of gas atoms released to the grain boundary is affected by these two processes. Furthermore, the matrix concentration is related to the number of gas atoms contained in the intergranular bubbles in that the former is influenced by the number of gas atoms continuously injected back into the matrix by the re-solution from the intergranular bubbles. By contrast, the latter, the number of gas atoms contained in the intergranular bubbles is determined by the matrix concentration, the former. That is, the former and the latter are inter-dependent. Therefore, in order to calculate the distribution of fission gas between the matrix and grain face, this interaction must be treated quantitatively.

Another common drawback of existing models is that most of them considered the formation of open tunnels at grain edges, through which gas atoms escape to the open space of fuel rod, in a rather simple way [2, 3]. They assumed that release path at grain edge is established suddenly at the moment that grain edge swelling due to gas bubbles reaches some experimentally or theoretically pre-determined value. This means that the gas release actually occurring before grain edge swelling reaches the pre-determined value can not be considered in their models.

Consequently, with emphasis given to the two points mentioned above, a new model is developed in this paper to describe the release behavior of fission gas and gaseous swelling at temperatures below approximately 1700°C where grain growth of UO_2 fuel is not expected to occur. The model introduces the concept of continuous formation of open tunnels at grain edges, where the degree of formation is proportional to the grain edge swelling. This enables to treat the continuous gas release through open tunnels from the beginning of life of fuel. In addition, the model describes analytically the amount of fission gas atoms released to grain boundary considering the interaction between the matrix and grain face concentration of gas atoms.

2. Model Development

2.1. Intragranular Behavior

It is a generally observed phenomenon that fission gas bubbles are not very mobile under most normal operating conditions and gas atom migration is the dominant mechanism by which gas reaches grain boundary [4]. In addition, it is commonly observed [5] that after a short period of irradiation the intragranular structure of UO_2 is decorated by a population of small bubbles with radius of about $10^{-9}m$ (10Å). Also it has been found out that under any particular set of operating conditions, power density, temperature etc., these bubbles stabilize in such a way that concentration of bubbles remains invariant under further irradiation. Under these circumstances, the rate equations that determine the concentration of gas in dynamic solution and the amount precipitated into intragranular bubbles are expressed by

$$\frac{dc}{dt} = \beta - \frac{dm}{dt} - \frac{dg_b}{dt} , \quad (1)$$

$$\frac{dm}{dt} = g_i c - b_i m , \quad (2)$$

where

c = concentration of gas in dynamic solution (atom/m^3)

m = concentration of gas in bubbles (atom/m^3)

g_b = concentration of gas atoms released to the grain boundary (atom/m^3)

β = gas production rate = 0.3 F (atom/m^3 · s)

F = fission density (fissions/m^3 · s)

g_i = $4\pi DC_B\rho_i$
= probability per second of gas atoms in dynamic solution being captured by bubble of radius ρ_i at any time t (s^{-1})

D = gas atom diffusion coefficient in the fuel lattice (m^2/s)

ρ_i =average radius of intragranular bubble (m)

C_B =number of intragranular bubbles of radius ρ_i ($1/m^3$)

b_i =intragranular re-solution parameter (s^{-1})

a =grain radius (m).

It should be emphasized here that the relation for g_i given above is based on two major simplifications [6]. The first one is the quasi- stationary approximation. The second one is that the radius of spherical intragranular bubble ρ_i is very small compared to the distance R separating the intragranular bubbles, that is $\rho_i/R \ll 1$ (see Fig. 1). Since steady-state condition is being treated in this paper, the first simplification is satisfied automatically. According to Baker's observation [7], the radius of spherical bubble is small compared to the distance between the bubbles as can be confirmed in Eq.(3) given below. Therefore, the second simplification also can be regarded as being satisfied.

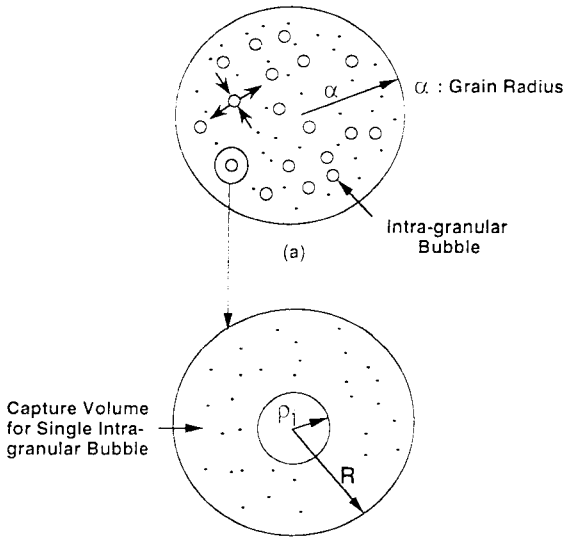

Fig. 1(a). Intra-granular Fission Gas Bubbles in the Matrix and

(b). the Unit Cell for Fission Gas Atom Absorption by the Intra-Granular Bubble.

White and Tucker [8] described the Baker's [7] observation of bubble density C_B by the following analytical formula :

$$C_B = 1.52 \times 10^{27} / T - 3.3 \times 10^{23} \quad (m^{-3}), \qquad (3)$$

where T is fuel temperature in K.

For very small bubbles, the internal pressure due to surface tension restraint is so high that the gas behavior deviates considerably from the ideal gas law, and the van der Waal's equation of state becomes more appropriate. It is assumed that the bubble in the matrix is in mechanical equilibrium with the bulk solid subjected to external hydrostatic stress σ_r. Then the volume of a gas atom V_1 contained in a bubble of radius ρ_i is

$$V_1 = B + \left[\left(\frac{2\gamma}{kT}\right)\frac{1}{\rho_i} + \frac{\sigma_r}{kT} \right]^{-1}, \qquad (4)$$

where B and γ are taken to be 85Å^3/atom and 1 N/m, respectively [6]. Under most steady-state operating conditions where only rod internal pressure exists, external hydrostatic stress σ_r is less than around 150 *atm (atmospheric pressure)* and the radius of intragranular bubbles is usually less than about 30Å as calculated by the present model. Under this situation, since the first term in the bracket of Eq.(4) is much larger than the second term, Eq.(4) can be simplified as

$$V_1 = B + \frac{kT}{2\gamma}\rho_i .$$

Since $kT/2\gamma \simeq 1$Å^2 at all temperatures of interest in reactor fuel operation [6], V_1 can be given by

$$V_1 = B + \rho_i \cdot 1\,\text{Å}^2 \quad (\text{Å}^3).$$

The number of gas atoms n_i contained in a bubble whose radius ρ_i is smaller than about 30Å can be expressed approximately as [6]

$$n_i = \frac{m}{C_B} = \left(\frac{4\pi\rho_i^3}{3}\right)\frac{1}{V_1} = \left(\frac{4\pi\rho_i^3}{3}\right)\frac{1}{B + \rho_i \cdot 1\,\text{Å}^2} . \qquad (5)$$

From Eq.(5), the following cubic equation for the radius of intragranular bubble is derived:

$$4\pi C_B \rho_i^3 - 3m\rho_i \cdot 1\,\text{Å}^2 - 3mB = 0 \ . \qquad (6)$$

A real root of Eq.(6) that exists under the condition of q^3+r^2 being greater than zero, which is found to be satisfied at all temperatures of interest, is given by

$$\rho_i = \left[\ r+(q^3+r^2)^{\frac{1}{2}} \right]^{\frac{1}{3}} + \left[\ r-(q^3+r^2)^{\frac{1}{2}} \right]^{\frac{1}{3}} \ (\text{Å}) \ , \qquad (7)$$

where

$$r = \frac{1}{2}\left(\frac{3m\cdot 85}{4\pi C_B}\right) \ \text{and} \ q = -\frac{1}{3}\left(\frac{3m}{4\pi C_B}\right) .$$

Two assumptions are introduced to describe the irradiation-induced grain boundary re-solution. First, a flux of gas atoms is induced to be ejected to an average distance λ from the grain face through the action of irradiation-induced re-solution. Second, only the grain boundary surface covered with gas bubbles is influenced by the re-solution (see Fig. 2). Then the net rate of fission gas release from the matrix to the grain boundary per unit time and unit area under

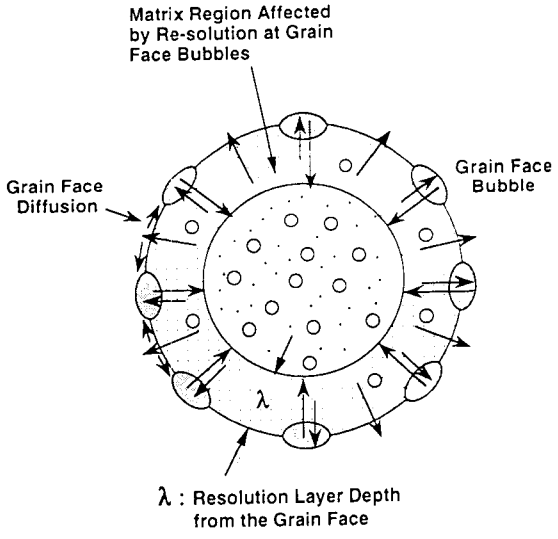

Fig. 2. Representation of Irradiation-Induced Resolution at Grain Face.

re-solution, dN_g/dt, is expressed by

$$\frac{dN_g}{dt} = F_o[\ 1-f_b\, b_f(b_i+g_i)N_g\lambda/2Db_i\beta t] \ , \qquad (8)$$

where

F_o = release flux to grain face without the action of the irradiation-induced re-solution

$$= 2\beta\left[\ \frac{Db_i t}{\pi(b_i+g_i)}\ \right]^{1/2} - \frac{\beta D b_i t}{a(b_i+g_i)} \quad [\ 9]$$

f_b = fraction of grain face covered by gas bubbles as defined by Eq.(19)

b_f = intergranular re-solution parameter (s^{-1})

λ = re-solution layer depth from the grain face (m).

The analytical solution of Eq.(8) is

$$N_g(t) = \frac{2\beta D b_i}{f_b\, b_f(b_i+g_i)\lambda}\left[\ 2t-\frac{2}{A}t^{1/2} + \frac{2}{A^2}(1-e^{-At^{1/2}}) + \frac{2a}{f_b b_f \lambda}(1-e^{\frac{f_b b_f \lambda t}{2a}})\right] \qquad (9)$$

where $A = 2\left[\ \frac{f_b^{\,2} b_f^{\,2}(b_i+g_i)\lambda^2}{\pi D b_i}\ \right]^{1/2}$.

From the assumption that fission gas atoms released to the grain face are distributed uniformly over the grain face area, the following relation is obtained between dg_b/dt and dN_g/dt:

$$\frac{dg_b}{dt} = \left(\frac{3}{a}\right)\frac{dN_g}{dt} \ . \qquad (10)$$

Substitution of Eq.(8) into Eq.(10) with the initial condition of $g_b(0)=0$ gives

$$g_b = \frac{6\beta D b_i}{a\, f_b\, b_f(b_i+g_i)\lambda}\left[\ 2t-\frac{2}{A}t^{1/2}+\frac{2}{A^2}(1-e^{-At^{1/2}}) + \frac{2a}{f_b b_f \lambda}(1-e^{\frac{f_b b_f \lambda t}{2a}})\right] \qquad (11)$$

Eqs.(1) to (11) can be solved numerically to obtain the amount of fission gas contained in both the matrix and the intragranular bubbles, and the amount released to the grain boundary as a function of ir-

radiation conditions and time.

For a van der Waal's gas, the swelling due to intragranular bubbles is given by

$$\left(\frac{\Delta V}{V}\right)_i = \frac{4\pi \rho_i^3 C_B}{3} . \quad (12)$$

The diffusion coefficient of fission gas $D(m^2/s)$ used here is given in Ref. 10:

$$D = 7.6 \times 10^{-10} \exp(-7 \times 10^4/RT) + s^2 j_v V' + 2 \times 10^{-40} F , \quad (13)$$

2.2. Intergranular (Grain Face) Behavior

For the treatment of gas release from grain face to grain edge, a more realistic grain shape must be used instead of assuming that grain shape is spherical. In this paper, it is assumed that UO_2 grain face is composed of fourteen identical circular faces [11]. The grain edge porosity in this shape is represented by a triangulated tube around the circumference of the grain face as can be seen in Fig. 4. Hence the name of this model is the "toroid" model. In addition, a grain edge bubble is shared by three neighboring grains and is bounded by three identical circular faces. The gas atoms collected there are assumed to be distributed evenly so that the circular edges form a torus where the fission gas atoms are stored. The equivalence in volume between the toroid and the spherical grain model gives the following relationship [8]:

$$r_{gf} = 0.5557\, a , \quad (14)$$

where r_{gf} is the radius of a circular grain face in the toroid model (see Fig. 3). For triangulated tunnels of radius of curvature ρ_e and semi-dihedral angle $\theta = 50°$, the fraction of grain edge area occupied by tunnels is given by [8]

$$\left(\frac{\Delta S}{S}\right)_e = 1.29\left(\frac{\rho_e}{a}\right) - 0.6041\left(\frac{\rho_e}{a}\right)^2 . \quad (15)$$

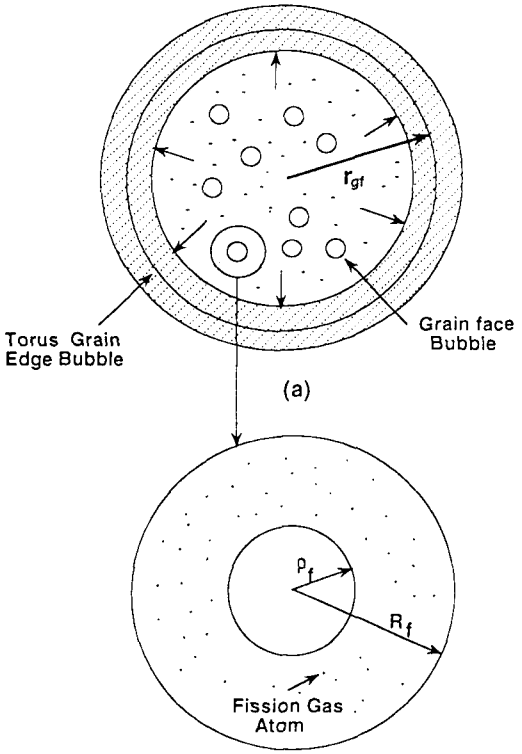

Fig. 3(a). Fission Gas Bubbles at the Grain Face and (b). the Unit Cell for the Capture of Gas Atoms by a Grain Face Bubble.

Fission gas atoms produced during the irradiation of UO_2 fuel diffuse through matrix until they encounter grain boundary, where they tend to precipitate into lenticular bubbles. It is necessary, therefore, to consider the nucleation and growth of the population of grain face bubbles. This bubble population will inhibit gas release and contribute to fuel swelling. Here a model is introduced for the grain face bubbles by assuming that the concentration of grain face bubbles is only a function of temperature given by Eq.(18). These bubbles are allowed to grow according to the rate of arrival of gas atoms at the grain face. As soon as a chosen fraction of grain face area

is covered by bubbles, all the gas atoms reaching the grain face are assumed to be released to the grain edge.

Observation of the fracture surfaces of UO_2 fuel reveals that grain face bubbles exhibit a remarkable uniformity of both size and spacing at least during the early stages of irradiation. Tucker [12] also justified the use of uniformly sized grain face bubbles in the modeling of fission gas release and swelling in UO_2 fuel. Therefore, it is assumed furthermore that the gas atoms arriving on a grain face are equally distributed among the fixed concentration of grain face bubbles. Then under these circumstances, where the enhancement of gas release due to grain growth that is known to occur above about 1700°C not being considered, the rate equations that account for the concentration of fission gas atoms on the grain face and the amount of fission gas on a grain face bubble are described as follows before grain face saturation is achieved :

$$\frac{dC_f}{dt} = 2\left(1 - f_b - \left(\frac{\triangle S}{S}\right)_e\right)\frac{a}{3}\frac{dg_b}{dt} - N_f g_f C_f \quad (16)$$

and

$$N_f \frac{dm_f}{dt} = N_f \cdot 2\pi\rho_f^2 \sin^2\theta \frac{a}{3}\frac{dg_b}{dt} + N_f g_f C_f \quad (17)$$

where

C_f = concentration of fission gas atoms on a grain face (atoms/m^2)

N_f = concentration of grain face bubbles (bubbles/m^2)

g_f = probability per second of fission gas atoms in solution on the grain face being captured by a grain face bubble of radius ρ_f at any time (m^2/bubble·s)

$$= \frac{2\pi D_s}{\ln\left[\frac{1}{(\pi N_f)^{1/2}\rho_f}\right]} \quad [1]$$

D_S = diffusion coefficient of fission gas in the grain surface (m^2/s)

m_f = number of fission gas atoms in a bubble of radius ρ_f (atoms/bubble).

Once the saturation of grain face by gas bubbles is achieved, all gas atoms arriving at grain boundary are assumed to be released to the grain edge. Therefore, after the grain face saturation, C_f and m_f remain unchanged just maintaining the values for the saturation state.

The concentration of grain face bubbles has been experimentally observed to fall with increasing temperature [13] :

$$N_f = 3.587 \times 10^8 \exp\left[\frac{1.327 \times 10^4}{T(K)}\right] \quad (\text{bubbles/m}^2) \quad . \quad (18)$$

At temperatures lower than 1300K, the concentration is given an upper limiting value of 10^{14} bubbles/m^2 [14].

Since the projected radius of grain face bubble is $\rho_f \sin\theta$, the fraction of grain face f_b covered by the gas bubbles is

$$f_b = N_f(\pi\rho_f^2 \sin^2\theta) \quad , \quad (19)$$

where ρ_f is the radius of grain face bubble.

There are several observations about when grain face saturates by gas bubbles. According to White and Tucker [8], the maximum fraction of grain face covered with bubbles is about 0.25. Hayns and Wood [2] assumed that the maximum coverage is 0.50. On the other hand, Tucker [22] asserted that typically a maximum coverage of around 0.70 is observed. If we denote the maximum coverage as f_b^{max}, the radius of grain face bubble required for grain face saturation ρ_f^{max} is

$$\rho_f^{max} = \left(\frac{f_b^{max}}{N_f \pi \sin^2\theta}\right)^{1/2} \quad . \quad (20)$$

Therefore, if the radius of grain face bubble is less than this value, no release from the grain face to the grain edge occurs except direct release from matrix to grain edge. After the grain face saturation, however, all the gas atoms arriving at the grain face are assumed to be released to the grain edge.

The volume of a grain face bubble is given by [8]

$$V_{gf} = \frac{4}{3}\pi\rho_f^3 f_f(\theta) \ , \tag{21}$$

where $f_f(\theta) = 1 - \frac{3}{2}\cos\theta + \frac{1}{2}\cos^3\theta$.

It is assumed that the pressure of gas pressure is always balanced by the sum of lattice surface tension and local hydrostatic stress ; that is, bubbles are always in equilibrium. It is also assumed that the supply of vacancies to the bubbles is sufficient to constrain the bubble growth to the limitation of gas atom supply. Then, assuming ideal gas law, the number of gas atoms m_f in a bubble of radius ρ_f required for mechanical stability is

$$m_f = P\,V_{gf}/kT = \frac{4\pi\rho_f^3}{3kT} f_f(\theta)\left(\frac{2\gamma}{\rho_f} + \sigma_r\right) , \tag{22}$$

where σ_r is the external hydrostatic stress on fuel pellet. Then Eq.(22) can be written as

$$\rho_f^3\left(1 + \frac{2\gamma}{\sigma_r\rho_f}\right) = \frac{3kTm_f}{4\pi f_f(\theta)\,\sigma_r} \ . \tag{23}$$

Since r is a physical constant and σ_r can be obtained from fuel rod internal pressure and contact pressure if PCI exists, the right-hand side of Eq.(23) can be regarded as constant once m_f is determined. Then the radius of grain face bubble ρ_f can be calculated depending on the relative magnitudes of 1 and $2r/\sigma_r\rho_f$. That is, in cases that 1 is very smaller or larger than $2r/\sigma_r\rho_f$, $1+2r/\sigma_r\rho_f$ can be reduced to 1 or $2r/\sigma_r\rho_f$, respectively. If 1 is comparable to $2r/\sigma_r\rho_f$, Eq.(23) can not be simplified and so the cubic equation must be solved. For convenience, however, it is assumed that the above three cases can be reduced to the following two cases depending on whether 1 is smaller than $2r/\sigma_r\rho_f$ or not.

The fractional volume swelling of the grain face bubbles, normalized to unit volume of grain matrix, can be computed by

$$\left(\frac{\Delta V}{V}\right)_f = \frac{1}{2}\frac{4\pi a^2 N_f}{4\pi a^3/3}\left(\frac{4}{3}\pi\rho_f^3 f_f(\theta)\right) . \tag{24}$$

In the above equation, the factor 1/2 is required since a grain face bubble is shared by two neighboring grains.

1) $1 \ll 2r/\sigma_r\rho_f$ (ρ_f is relatively small)

In the beginning of reactor operation, the radius of grain face bubble ρ_f would be very small due to the small amount of fission gas released to the grain boundary. In this case, $2r/\sigma_r\rho_f$ is much greater than 1 and hence Eq.(23) can be simplified as

$$\rho_f^2 = \frac{3kTm_f}{8\pi\gamma f_f(\theta)} \ . \tag{25}$$

Therefore, ρ_f is expressed as

$$\rho_f = \left(\frac{3kTm_f}{8\pi\gamma f_f(\theta)}\right)^{1/2} . \tag{26}$$

By inserting Eq.(26) into Eq.(24), the swelling due to grain face bubbles is obtained by

$$\left(\frac{\Delta V}{V}\right)_f = \frac{3\pi N_f f_f(\theta)}{2}\left(\frac{3kTm_f}{8\pi\gamma f_f(\theta)}\right)^{3/2} . \tag{27}$$

2) $1 \gg 2r/\sigma_r\rho_f$ (ρ_f is relatively large)

As irradiation of fuel continues, ρ_f would become larger due to the increased amount of fission gas released to the grain boundary and the time would be reached when $2r/\sigma_r\rho_f$ is much smaller than 1. Then Eq.(23) can be simplified as follows :

$$\rho_f^3 = \frac{3kTm_f}{4\pi f_f(\theta)\,\sigma_r} \ . \tag{28}$$

Therefore, ρ_f is expressed as

$$\rho_f = \left(\frac{3kT}{4\pi f_f(\theta)\,\sigma_r}\right)^{1/3} m_f^{1/3} . \tag{29}$$

Inserting Eq.(28) into Eq.(24) gives the swelling due to grain face bubbles as

$$\left(\frac{\Delta V}{V}\right)_f = \frac{3kT}{2a\sigma_r} N_f m_f \ . \tag{30}$$

According to Reynolds [15], surface diffusion coefficient D_s (m^2/s) is

$$D_s\gamma = 560\exp(-Q/RT) , \tag{31}$$

where Q is 119 kcal.

Eqs.(16), (17), (26) and (29), and (27) and (30) are solved numerically to obtain the amount of gas contained both on the grain face and in the grain face bubble, the radius of grain face bubble, and the swelling due to grain face bubbles.

2.3. Grain Edge Behavior

It is assumed that release rate of fission gas from grain edges to open space is proportional to both the instantaneous fission gas inventory at the grain edges and the fraction of grain edge bubbles interlinked to open spaces. Before grain face saturation is achieved, direct release from the matrix to the grain edge only exists. In addition, since a triangulated grain edge bubble is shared by three neighboring grains as shown by Fig. 4 and is bounded by three equivalent spherical surfaces, the rate equation describing the concentration of fission gas atoms along the grain edge bubble is expressed as follows before grain face is saturated:

$$2\pi r_{gf}\frac{dC_e}{dt} = 3(1-f)\pi r_{gf}^2\left(\frac{\triangle S}{S}\right)_e \frac{a}{3}\frac{dg_b}{dt} \quad (32)$$

where

C_e = fission gas atom concentration along grain edge (atom/m)

f = fraction of grain edge bubbles interlinked to open surfaces that would be discussed in Sec. 2.4.

Using Eq.(14), Eq.(32) can be reduced as

$$\frac{dC_e}{dt} = (1-f)\,0.278\,a^2\left(\frac{\triangle S}{S}\right)_e \frac{dg_b}{dt} . \quad (33)$$

After grain face saturation, the rate equation for the grain edge concentration can be expressed as follows based on the assumption of Sec. 2.2 that all the gas atoms arriving at grain boundary are released to the grain edge:

$$2\pi r_{gf}\frac{dC_e}{dt} = 3(1-f)\pi r_{gf}^2\frac{a}{3}\frac{dg_b}{dt} . \quad (34)$$

Using the relation of Eq.(14), Eq.(34) can be expressed by

$$\frac{dC_e}{dt} = (1-f)\,0.278\,a^2\frac{dg_b}{dt} . \quad (35)$$

Then the equation for the number of gas atoms in a grain edge bubble (circular torous in the "toroid" model) m_e is given by

$$m_e = 2\pi r_{gf} C_e . \quad (36)$$

As in the case of grain face bubble, the pressure of gas bubble is assumed to be always balanced by the lattice surface tension and the local hydrostatic stress. Also it is assumed that grain edge bubbles receives sufficient vacancies to enable them to grow as equilibrium gas bubbles limited by the arrival rate of stable gas atoms. Then the number of gas atoms m_e required for mechanical stability in a triangulated

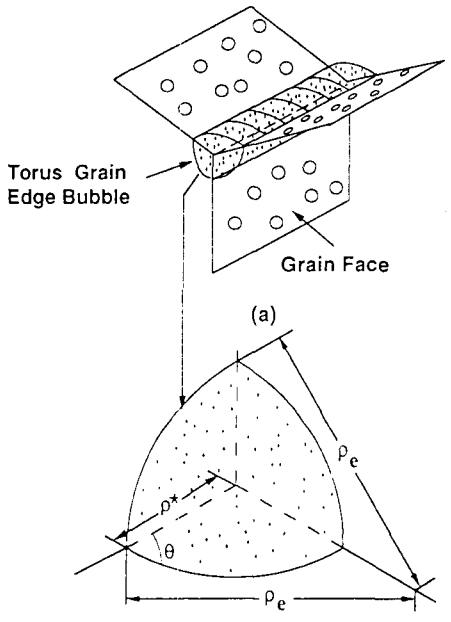

ρ*: Equivalent radius of tri-angulated grain edge bubble
ρe: Radius of curvature of grain edge bubble
θ: Semi di-hedral angle

Fig. 4. Schematic Diagram of a Torous Grain Edge Bubble
(a) Side View and (b) Cross-Sectional View.

grain edge bubble of radius of curvature ρ_e is calculated from

$$m_e = \frac{V_e}{kT}\left(\frac{2\gamma}{\rho_e} + \sigma_r\right), \quad (37)$$

where

$$V_e = 2\pi r_{gf}\{\pi\rho_e^2 f_t(\theta)\}$$

$$f_t(\theta) = \frac{3}{\pi}\left\{\theta - \frac{\pi}{6} - 2\cos\theta\cdot\sin(\theta - \frac{\pi}{6})/\sqrt{3}\right\}$$ [8]

=factor which relates the cross-sectional area of a triangulated tunnel to that of a circular tunnel of the same radius of curvature.

Combination of Eq.(36) with Eq.(37) gives

$$\rho_e^2\left(1 + \frac{2\gamma}{\sigma_r\rho_e}\right) = \frac{kTC_e}{\pi f_t(\theta)\sigma_r}. \quad (38)$$

As in the case of Eq.(23), ρ_e is determined depending on the relative magnitudes of 1 and $2r/\sigma_r\rho_e$.

The fractional volume swelling of the grain edge bubbles, normalized to unit volume of grain matrix, can be computed from

$$\left(\frac{\Delta V}{V}\right)_e = \frac{1}{3}\,14\,\frac{1}{4\pi a^3/3}\,2\pi r_{gf}\{\pi\rho_e^2 f_t(\theta)\}$$

$$= \frac{7\pi}{a^3} r_{gf}\rho_e^2 f_t(\theta). \quad (39)$$

where the factors 1/3 and 14 are introduced because a grain edge bubble is shared by three neighboring grains and there are 14 circular faces per grain, respectively.

1) $1 < 2r/\sigma_r\rho_f$ (ρ_f is relatively small)

In the beginning of reactor operation, the radius of grain edge bubble ρ_e would be very small and hence Eq.(38) would result in

$$\rho_e^2\frac{2\gamma}{\sigma_r\rho_e} = \frac{kTC_e}{\pi f_t(\theta)\sigma_r},$$

which leads to

$$\rho_e = \frac{kTC_e}{2\pi\gamma f_t(\theta)}. \quad (40)$$

Inserting Eqs.(14) and (40) into Eq.(39) gives

$$\left(\frac{\Delta V}{V}\right)_e = \frac{12.22\, f_t(\theta)}{a^2}\left(\frac{kTC_e}{2\pi\gamma f_t(\theta)}\right)^2. \quad (41)$$

2) $1 < 2r/\sigma_r\rho_f$ (ρ_f is relatively large)

As irradiation of fuel goes on, ρ_e would become larger due to the increased amount of fission gas released to the grain boundary and the time would be reached when $2r/\sigma_r\rho_e$ (ρ_e is much smaller than 1. From that moment, Eq.(38) can be simplified as

$$\rho_e^2 = \frac{kTC_e}{\pi f_t(\theta)\sigma_r},$$

which reduces to

$$\rho_e = \left(\frac{kTC_e}{\pi f_t(\theta)\sigma_r}\right)^{1/2}. \quad (42)$$

Inserting Eqs.(14) and (42) into Eq.(39) gives

$$\left(\frac{\Delta V}{V}\right)_e = \frac{3.89}{a^2}\frac{kTC_e}{\sigma_r}. \quad (43)$$

Eqs.(33), (35), (40), (42), (41) and (43) are solved numerically to obtain the amount of gas contained in the grain edge bubble, the radius of grain edge bubble, and the swelling due to grain edge bubbles.

2.4. Incubation Period for Interlinkage at Grain Edge

According to Sontheimer et al. [16], the least volume (threshold volume) of fission gas atoms required for gas bubble interlinkage at grain boundary is $10^{-6}m^3(STP)/m^3$ at a hydrostatic pressure of 23 *atm*. Then the total number of gas atoms on grain edge at this situation is $\{\pi r_g^2 - \pi(r_g - \rho^*)^2\}\cdot 10^{-6}m^3(STP)$, where ρ^* is the equivalent radius of triangulated grain edge bubble (see Fig. 4). The radius ρ^* is obtained from the relation that the cross-sectional area of the bubble $\pi\rho_e^2 f_t(\theta)$ is equal to $\pi\rho^{*2}$. If we convert the above threshold volume into that corresponding to operating temperature and pressure, then the volume V_e^o is given by

$$V_e^o = \frac{P_S T}{P T_S}\{\pi r_{gf}^2 - \pi(r_{gf} - \rho^*)^2\}\cdot 10^{-6}\ (m^3), \quad (44)$$

where P_S T_S are 2.3 *MPa* and 298*K*, respectively. Then the following relation would be satisfied when the incubation of grain edge is established :

$$V_e^o = 2\pi r_{gf} C_e \frac{V_m}{N_{AV}} , \quad (45)$$

where V_m is the volume of one mole gas ($0.0224\,m^3$) and N_{AV} is the number of atoms in one mole gas (6.023×10^{23}). Therefore, the concentration of gas atoms at grain edge at the moment that incubation of grain edge is completed, C_e^{inc}, is

$$C_e^{inc} = \frac{N_{AV}}{2\pi r_{gf}} \frac{V_e^o}{V_m} \quad (46)$$

1) $1 < 2r/\sigma_r\rho_e$ (ρ_e is relatively small)

In case that ρ_e is relatively small and the relationship $1 < 2r/\sigma_r\rho_e$ is satisfied, combination of Eqs.(41) and (46) gives the minimum swelling $(\Delta V/V)_e^{min}$ that are required to form a release path at the grain edge :

$$\left(\frac{\Delta V}{V}\right)_e^{min} = \frac{12.22\ f_t(\theta)}{a^2} \left(\frac{kT C_e^{inc}}{2\pi\gamma f_t(\theta)}\right)^2 . \quad (47)$$

2) $1 < 2r/\sigma_r\rho_e$ (ρ_e is relatively small)

In case that ρ_e is relatively large and the relationship $1 < 2r/\sigma_r\rho_e$ is satisfied, combination of Eqs.(43) and (46) gives the minimum swelling $(\Delta V/V)_e^{min}$ that are required to form a release path at the grain edge :

$$\left(\frac{\Delta V}{V}\right)_e^{min} = \frac{3.89}{a^2} \frac{kT C_e^{inc}}{\sigma_r} . \quad (48)$$

2.5. Interlinkage at Grain Edge

It is well known that, as residence time and fuel temperature increase, networks of channels are established at grain edges and that fission gases are released through some of these channels connected to the open space of fuel. Many attempts have been made so far to correlate, both theoretically and by observation, grain edge swelling to the extent of formation of grain edge tunnel. Tucker and Turnbull [17] have shown theoretically that a stable tunnel network forms when the swelling at grain edges is greater than 5%. Turnbull [18] shown experimentally that tunnels form when the swelling is greater than 7%. Beere and Reynolds [19] predicted that tunnel is established when the swelling at grain edges is greater than 8%. Based on these works, many models assumed that release pathways at grain edges are achieved suddenly at the moment that grain edge swelling due to gas bubbles reaches some preassigned value. According to percolation theory [31], however, networks such as grain edge tunnels have non-zero probability of being open at any instant of time. Hence a long range interlinkage among grain edge tunnels would be established at fractional swelling less than the above-mentioned threshold values at which all tunnels are suddenly interlinked to the fuel open space. These approaches, therefore, have a common drawback that they did not taken into account the fact that gas release takes place actually even before the grain edge swelling reaches some threshold value.

Based on the above argument, it is assumed in this paper that the fraction of grain edge bubbles interlinked to the fuel open space, f, depends on the grain edge swelling. It is evident that f should increase from a value of zero as the grain edge swelling $(\Delta V/V)_e$ increases. For this reason f is proposed as follows :

$$f = \begin{bmatrix} 0 \text{ for } \left(\frac{\Delta V}{V}\right)_e = \left(\frac{\Delta V}{V}\right)_e^{min} \\ 1 \text{ for } \left(\frac{\Delta V}{V}\right)_e = \left(\frac{\Delta V}{V}\right)_e^{max} \end{bmatrix} \quad (49)$$

Then as was done by Sontheimer et al.[16] and as was supported by experiments [20], the dependence of f on $(\Delta V/V)_e$ between 0 and 1 is defined as follows :

$$f = \quad (50)$$

$$\left\{\left(\frac{\Delta V}{V}\right)_e - \left(\frac{\Delta V}{V}\right)_e^{min}\right\} / \left\{\left(\frac{\Delta V}{V}\right)_e^{max} - \left(\frac{\Delta V}{V}\right)_e^{min}\right\}$$

In addition, once grain edge tunnels are developed, they are assumed to be stable and hence continue to provide release pathways. After maximum grain edge swelling is achieved, all the gas atoms that reach the grain edges are assumed to be released to the fuel outside.

2.6. Fission Gas Release

1) Release via Interlinked Tunnel

The amount of fission gas released to open space through interlinked grain edge tunnels should be calculated by considering whether grain face is saturated by gas bubbles or not. Before grain face is saturated, gas release rate R_e is

$$R_e = \frac{1}{3} \cdot 14 \cdot f \cdot 3\pi r_{gf}^2 \left(\frac{\triangle S}{S}\right)_e \frac{a}{3} \frac{dg_b}{dt} \quad . \tag{51}$$

where again the factors 1/3 and 14 are introduced for the same reason given for Eq.(39).

After the grain face is saturated, all gas atoms released to the grain boundary would migrate to the grain edge. Therefore, gas release rate through interlinked grain edge tunnel is

$$R_e = \frac{1}{3} \cdot 14 \cdot f \cdot 3\pi r_{gf}^2 \frac{a}{3} \frac{dg_b}{dt} \quad . \tag{52}$$

2) Release Due to Recoil and Knock-out

At low temperatures where gas atom mobility is very low, only the fission gases formed very close to an external surface can escape by the mechanisms of recoil and knock-out. These release mechanisms, which are independent of both temperature and its gradient, affect only the outer layer of the fuel (within about 10μm of the free surface). The release rate per unit fuel volume due to recoil and knock-out R_d is given by [21]

$$R_d = \frac{\gamma F}{4} \left(S_g \mu_g + 2 S_t \mu_u^{ko}\right), \tag{53}$$

where

γ = fission yield of stable fission products (0.3)
F = fission density (fissions/m^3 · s)
S_g = geometrical surface area of the fuel (m^2)
S_t = total surface area of the fuel (m^2)
μ_g = range of the fission fragment in the fuel (~10μm)
μ_u^{ko} = range of the higher-order uranium knock-on in UO_2 (~50 Å).

3) Total Release

Total release rate R_t of fission gas atoms to the fuel outside is the sum of the release rate R_e through interlinked grain edge bubbles and the release rate R_d due to recoil and knock-out. Therefore, R_t is

$$R_t = R_e + R_d \quad . \tag{54}$$

Before grain face is saturated by gas bubbles, the sum of Eqs.(51) and (53) gives the total release rate R_t:

$$R_t = \frac{1}{3} \cdot 14 \cdot f \cdot 3\pi r_{gf}^2 \left(\frac{\triangle S}{S}\right)_e \frac{a}{3} \frac{dg_b}{dt} + \frac{\gamma F}{4} \left(S_g \mu_g + 2 S_t \mu_u^{ko}\right) \tag{55}$$

On the other hand, after grain face is saturated, the total release rate R_t is obtained from the sum of Eqs.(52) and (53):

$$R_t = \frac{1}{3} \cdot 14 \cdot f \cdot 3\pi r_{gf}^2 \frac{a}{3} \frac{dg_b}{dt} + \frac{\gamma F}{4} \left(S_g \mu_g + 2 S_t \mu_u^{ko}\right) \tag{56}$$

3. Physical Parameters

Main physical parameters affecting fission gas release to grain boundary are temperature, volume diffusion coefficient, grain size, intra- and intergranular re-solution probabilities, and re-solution depth layer. According to Turnbull and Cornell [23], intragranular re-solution probability bi is around 3.0×10^{-4}. Intergranular re-solution probability b_g and re-solution layer

depth from the grain boundary λ are taken to be 1.0×10^{-5} and 1.0×10^{-8}, respectively [8]. Also the maximum fraction of grain face covered with gas bubbles f_b^{max} is assumed to be 0.25 [8]. Maximum grain edge swelling at which release paths are completed is given as 0.07 [18]. Table 1 shows the reference values used in the present parametric analysis. Temperature distribution along radial direction is calculated as a function of burnup and enrichment considering power depression with the use of FACTOR [24].

4. Pellet Division for Analysis

When the fuel pellets are subjected to temperature gradient, they crack both radially and axially when a threshold power level is exceeded. According to Notley [26], it is assumed that a fuel pellet is composed of two regions depending on its temperature distributions : (a) an inner plastic region whose temperature is greater than 1400°C and (b) an outer region containing a number of radial cracks through which gas release can occur. Oguma [27] has shown that the number of pellet cracks increase almost linearly with the linear power of fuel rod and the number of radial fuel cracks is about one-half of the linear power (in kW/m). In addition, according to Merckx [30], axial cross section of a pellet ramped to a nominal operational power shows three to four circumferential cracks along axial direction of a pellet. Based on these observations, the schematic geometry of a fuel pellet during irradiation can be ideally represented as in Fig. 5. Therefore, once the fuel rod power and pellet dimensions are given, the total surface area available for fission gas release by recoil and knock-out can be calculated.

Table 1. Physical Parameters

Parameter	Value
• Maximum grain edge swelling, $(\Delta V/V)_e^{max}$	0.07
• Maximum coverage of grain face by bubbles, f_b^{max}	0.25
• Intragranular re-solution probability, b_i	3.0×10^{-4}
• Intergranular re-solution probability, b_j	1.0×10^{-5}
• Re-solution depth layer, λ	1.0×10^{-8}

5. Comparison with Experimental Data

In this section, predictions of the present model are compared with experimentally observed gas release data for light water reactor (LWR) fuels using the physical constants given in Table 1. These constants are available in open literatures and are not adjusted to fit the measured data. Generally only a few data of the measured fission gas release are well characterized. Therefore, in cases that pertinent informations such as grain size, fuel surface temperature, radial power change as a function of burnup, etc. are not well specified, typical values for commercial LWR fuels are used for calculation.

To benchmark the present model, the first comparison is made with the U.K. Atomic Energy Authority (UKAEA) data [28]. These high burnup UO_2 data were reported for small diameter fuel rods irradiated in the U.K. Atomic Energy Authority reactor DIDO to about 45 MWd/kgU. The UO_2 specimens were irradiated at a fission rate that ranged from 2.75×10^{13} to 8.54×10^{13} fissions/cm^3 · s. The measured grain size and the fuel surface temperature were 15 m and ~600°C, respectively. The as-fabricated data and irradiation conditions are given in Table 2.

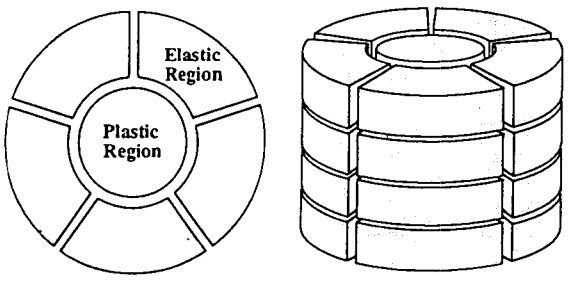

Fig. 5. Ideal Representation of a Cracked Fuel Pellet During Irradiation

Fig. 6 shows that the present model adequately predicts fission gas release for intermediate release range of 1 to 10%. But Fig. 7, which displays the ratio of calculated to measured release data as a function of fuel centerline temperature, indicates another aspect of the present model. For higher centerline temperatures greater than about 1400°C, though data points are not enough to draw any clear conclusion, the

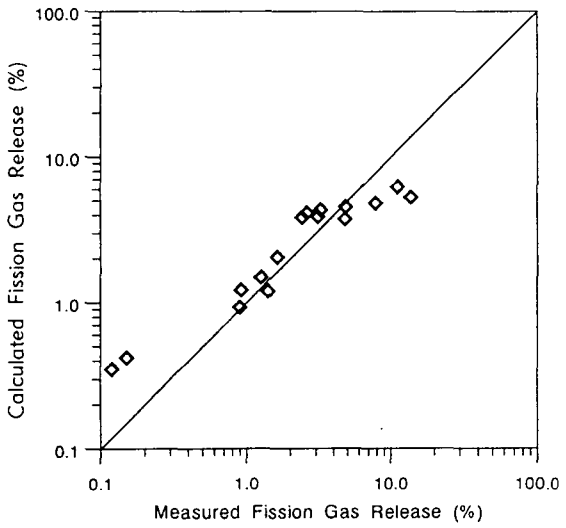

Fig. 6. Comparison Between the Calculated and the UKAEA Fission gas release data

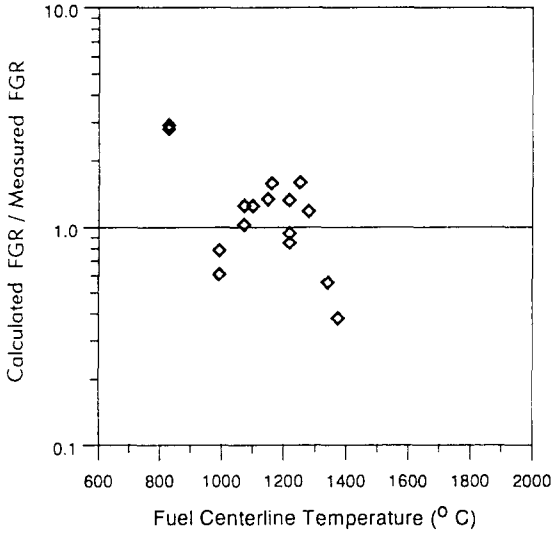

Fig. 7. Comparison Between the Calculated and the UKAEA Fission Gas Release Data Based on Fuel Centerline Temperature.

Table 2. UKAEA Fission Gas Release Data [28]

Pin No.	Pellet Diameter (mm)	Average Burnup (MWd/kgU)	Centerline Temperature (°C)	Fuel Density (% TD)	He Fill Gas Pressure (atm)	Release (%)
5020	5.94	7.40	1279	95.1	1.0	1.26
5027	6.56	9.40	1218	95.1	1.0	1.41
5028	5.94	10.0	1205	95.1	1.0	0.92
5036	5.94	16.2	1373	95.1	1.0	13.9
5026	4.82	17.9	1250	95.1	1.0	2.42
5042	4.82	27.8	1341	95.1	1.0	11.2
5040	3.70	34.2	1220	95.1	1.0	4.84
5034	4.26	12.1	1357	98.5	1.0	0.12
5033	4.70	12.6	1072	98.5	1.0	0.90
5031	3.64	14.2	1033	98.2	1.0	0.15
5019	5.82	17.4	1073	98.5	1.0	1.63
5041	4.70	29.8	1100	98.5	1.0	3.12
5022	3.74	32.3	1160	98.2	1.0	2.66
5039	3.64	36.6	1150	98.2	1.0	3.24
5050	3.74	41.7	1010	98.1	1.0	4.80
5049	3.74	44.2	1020	98.1	1.0	7.90

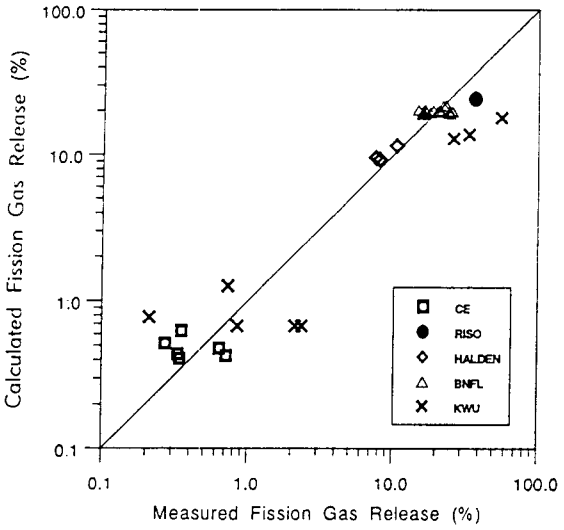

Fig. 8. Comparison Between the Calculated and the Measured fission Gas Release Data LWR Fuel

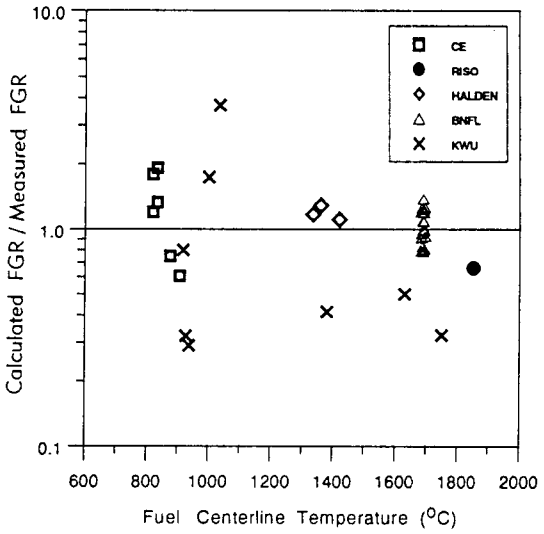

Fig. 9. Ratio of Measured to Calculated Fission Gas Release Data For LWR Fuel as a Function of Fuel Centerline Temperature.

model shows the tendency to underpredict the measured data. It seems that this tendency can be explained by the fact that the present model is developed based on the assumption that fission gases are released by only gas atom diffusion and gas bubbles are stationary. However, for fuel temperatures of higher than certain value, bubbles of gas atoms both in the matrix and on the grain face move along temperature gradient and this contributes to the fission gas release [6]. Furthermore, additional release due to grain growth at fuel temperatures greater than ~ 1700°C has not been treated, which is another main source of gas release. These two simplifications are likely to be the most probable cause for the underprediction of the present model for fuels with high centerline temperatures.

The second comparison is made with the experimental data obtained from various LWR fuel rods [29]. Since the detailed power history informations are not available, each rod was assumed to be irradiated by the constant average linear power of Table 3. Based on this assumption and other data of Table 3, fuel centerline temperatures were calculated for each data. Except for burnup, the as-fabricated data and the irradiation conditions for this comparison cover almost all the ranges found in LWR fuel rods; average linear heat rate of 9.0 to 44.2 kW/m, fuel density of 92.2 to 95.3% *TD*, fill gas pressure of 0.987 to 30.62 atm and grain size of 2.5 to 15m. Fig. 8 indicates that the present analysis shows no bias for five kinds of fuel. But as shown in Fig. 9, the model shows wide scatter band in the ratio of calculated to measured data for lower centerline temperatures. This tendency can be explained as follows: when the fuel centerline temperature is lower than about 1000°C, the dominant mechanism for fission gas release is direct recoil and knock-out. Then in this case, the sum of the area of geometrical surface and that of the surface created by cracks decides the amount of gas released to fuel outside, since the direct release occurs through these surfaces. Though one simplified approach was made at Sec. 4, it is very difficult to quantify the crack surface area since the cracking of UO_2 fuel is a complex phenomenon. This complexity and the very small fractional release which can cause measurement uncertainty may be the reason for large variation in the ratio of calcul-

Table 3. Fission Gas Release Data for LWR Fuel [29]

	Pellet Diameter (mm)	Burnup Peak/Average (MWd/kgU)	Linear Heat Peak/Average (kW/m)	Fuel Density (% TD)	He Fill Gas Pressure (atm)	Grain Size (μm)	Release (%)
CE							
46	9.64	23.8/21.6	36.4/22.0	93.0	30.62	15.0	0.71
47	9.64	32.0/29.1	36.4/20.7	93.0	30.62	15.0	0.64
50	9.64	21.4/18.7	29.9/19.0	95.0	30.62	4.0	0.33
51	9.64	28.6/25.8	29.9/18.4	95.0	30.62	4.0	0.35
01	9.64	21.4/18.7	29.9/9.00	93.0	30.62	2.5	0.27
05	9.64	28.6/25.8	29.9/18.4	93.0	30.62	2.5	0.34
RISO							
M2-2C	12.6	44.3/41.9	63.6/44.2	94.9	1.0	10.0	36.6
HALDEN							
432-1	10.7	22.2/20.2	44.9/35.9	95.0	1.0	10.0	7.50
432-5	10.7	22.2/20.0	46.3/35.3	92.0	1.0	10.0	8.00
432-6	10.7	22.2/20.0	44.9/35.4	92.0	1.0	10.0	10.05
BNFL							
1-BS	9.26	41.1/31.5	58.1/38.1	95.3	13.61	10.0	21.2
2-AZ	9.26	41.1/30.4	58.1/38.1	95.3	13.61	10.0	15.7
3-CM	9.26	41.1/32.7	58.1/38.1	95.3	13.61	10.0	15.8
4-CJ	9.26	41.1/31.1	58.1/38.1	93.4	13.61	10.0	24.0
5-DH	9.26	41.1/33.4	58.1/38.1	93.2	13.61	10.0	20.0
6-BR	9.26	41.1/31.8	58.1/38.1	93.2	13.61	10.0	15.7
7-DG	9.26	41.1/34.5	58.1/38.1	93.2	13.61	10.0	20.5
8-BC	9.26	41.1/33.4	58.1/38.1	93.4	1.0	10.0	25.3
9-CX	9.26	41.1/30.4	58.1/38.1	93.4	13.61	10.0	24.3
10-BT	9.26	41.1/32.8	58.1/38.1	93.2	13.61	10.0	25.4
11-CC	9.26	41.1/34.2	58.1/38.1	93.1	1.0	10.0	22.9
12-BG	9.26	41.1/32.8	58.1/38.1	93.4	1.0	10.0	16.3
13-AR	9.26	41.1/31.4	58.1/38.1	93.4	13.61	10.0	24.2
15-CL	9.26	41.1/31.7	58.1/38.1	93.2	1.0	10.0	17.8
16-BX	9.26	41.1/34.0	58.1/38.1	93.2	1.0	10.0	21.9
18-CF	9.26	41.1/31.9	58.1/38.1	95.3	1.0	10.0	14.7
19-BU	9.26	41.1/30.2	58.1/38.1	95.3	1.0	10.0	16.7
20-AD	9.26	41.1/31.7	58.1/38.1	95.3	1.0	10.0	18.6
KWU							
8610	9.1	34.5/30.1	24.8/17.6	94.4	0.987	10.0	2.34
5348	9.1	34.5/30.1	24.7/17.6	94.4	0.987	10.0	2.11
8613	9.1	34.5/30.1	24.8/17.6	94.4	0.987	10.0	0.85
2736	9.1	23.2/20.6	26.7/21.1	94.4	21.7	10.0	0.73
11159	9.1	12.4/11.1	27.9/22.1	94.4	21.7	10.0	0.21
150	9.1	22.5/19.9	46.8/36.4	92.2	27.6	10.0	25.9
45	9.1	42.6/38.1	45.9/35.3	92.2	27.6	10.0	55.5
98	9.1	35.1/31.4	36.5/29.0	92.2	27.6	10.0	33.2

ated gas release to measured data. But for intermediate centerline temperatures of 1000 to 1400°C, the agreement between calculation and measurement is reasonable except one data for KWU fuel because the gas released by direct recoil and knock-out is only the small fraction of the total released amount. Therefore, it can be concluded that the model developed in this paper shows reasonable agreement for fuel centerline temperatures of 1000 to 1400°C, wide scatter band for centerline temperatures lower than 1000°C, and underprediction for centerline temperatures higher than 1400°C.

Although accurate assessment of the present model against fission gas release data obtained for LWR fuel has to be made after it is incorporated into a well proven code, Figs. 13 to 16 show that the present model reasonably predicts the fission gas release for fuel centerline temperatures between 1000 to 1400°C, which is typical value for current LWR fuels.

6. Conclusions and Recommendation

A mechanistic model has been developed to predict the release behavior of fission gas during steady-state irradiation of LWR UO_2 fuel. Under the assumption that UO_2 grain surface is composed of fourteen identical circular faces and grain edge bubble can be represented by a triangulated tube around the circumference of three circular grain faces, it introduces the concept of continuous formation of open grain edges tunnels that is proportional to grain edge swelling. In addition, it takes into account the interaction between the gas release from matrix to grain boundary and the reintroduction of gas atoms into the matrix by irradiation- induced re-solution of grain face bubbles. It also treats analytically the behavior of intragranular, intergranular (grain face), and grain edge bubbles using the assumption that both intra- and intergranular bubbles are uniform in both radius and number density.

Parametric analysis has been performed to determine how the main physical parameters such as temperature, diffusion coefficient, and grain face bubble concentration influence the fission gas release. The analysis shows the trend that agrees with other fission gas release models found in the literature and experimental findings.

Comparison of the present model with experimental data shows that the model's prediction produces reasonable agreement for fuel with centerline temperatures of 1000 to 1400°C, wide scatter band for fuel with centerline temperatures lower than 1000°C, and underprediction for fuel with centerline temperatures higher than 1400°C.

It is recommended that the present model should be improved by considering the enhancement of fission gas release due to both bubble movement and grain growth at higher fuel temperatures. Furthermore, to analyze the performance of high burnup fuel whose average burnup is greater than about 50 MWd/kgU, additional release at rim region of fuel should be considered.

References

1. A. Villalobos, A. R. Wazzan, and D. Okrent, "Analysis of Fission Gas Disposition in Light Water Reactor Steady-State Operation," *Nucl. Tech.*, **58,** 492 (1982)
2. M.R. Hayns and M.H. Wood, "On the Rate Theory Model for Fission Gas Behavior in Nuclear Fuels," *J. Nucl. Mater.*, **59,** 293 (1976)
3. C.C. Dollins and F. A. Nichols, "Swelling and Gas Release in UO_2 at Low and Intermediate Temperatures," *J. Nucl. Mater.*, **66,** 143 (1977)
4. J. Weisman, P.E. Macdonald, A. Miller, and H.M. Ferrari, "Fission Gas Release from UO_2 Fuel Rods with Time Varying Power Histories," *Trans. Am. Nucl. Soc.*, **12,** 900 (1969)
5. R.M. Cornell, "The Growth of Fission Gas Bubbles in Irradiated Uranium Dioxide," *Phil. Mag.*, **19,** 539 (1969)

6. D.R. Olander, *Fundamental Aspects of Nuclear Reactor Fuel Elements,* TID-26711-P1 (Energy Research and Development and Administration, 1976) Chapeter 13.
7. C. Baker, "The Fission Gas Bubble Distribution in Uranium Dioxide from High Temperature Irradiated SGHWR Fuel Pins," *J. Nucl. Mater.*, **66,** 283 (1977)
8. R.J. White and M.O. Tucker, "A New Fission Gas Release Model," *J. Nucl. Mater.*, **118,** 1 (1983)
9. M.V. Speight, "A Calculation on the Migration of Fission Gas in Material Exhibiting Precipitation and Re-solution of Gas Atoms Under Irradiation," *Nucl. Sci. Eng.*, **37,** 180 (1969)
10. J.A. Turnbull et al., "The Diffusion Coefficients of Gaseous and Volatile Species During the Irradiation of Uranium Dioxide," *J. Nucl. Mater.*, **107,** 168 (1982)
11. M.O. Tucker, "A Simple Description of Interconnected Grain Edge Porosity," *J. Nucl. Mater.*, **79,** 199 (1979)
12. M.O. Tucker, "Relative Growth Rates of Fission Gas Bubbles on Grain Faces," *J. Nucl. Mater.*, **78,** 17 (1978)
13. C.T. Walker, P. Knappik and M. Mogensen, "Concerning the Development of Grain Face Bubbles and Fission Gas Release in UO_2 Fuel," *J. Nucl. Mater.*, **160,** 10 (1988)
14. J.R. Matthews and M.H. Wood, "A Simple Operational Gas Release and Swelling Model. II. Grain Boundary Gas," *J. Nucl. Mater.*, **91,** 241 (1980)
15. G.L. Reynolds, "The Surface Self-Diffusion of Uranium Dioxide," *J. Nucl. Mater.*, **24,** 69 (1967)
16. F. Sontheimer, P. Dewes, R. Manzel, and H. Stehle, "Release of the Volatile Fission Products Xe, Kr, and Cs from PWR Fuel Under Steady and Transient Conditions up to High Burnup," IAEA Technical Committee on Fuel Rod Internal Chemistry and Fission Product Behavior, Karlsruhe, Germany (1985)
17. M.O. Tucker and J.A. Turnbull, "The Morphology of Interlinked Porosity in Nuclear Fuels," *Proc. Roy. Soc.*, **343,** 229 (1975)
18. J.A. Turnbull, "The Effect of Grain Size on the Swelling and Gas Release Properties of UO_2 During Irradiation," *J. Nucl. Mater.*, **50,** 62 (1974)
19. W. Beere and G.L. Reynolds, "The Morphology and Growth of Interlinked Porosity in Irradiated UO_2," *J. Nucl. Mater.*, **47,** 51 (1973)
20. P. Knudsen, C. Bagger, H. Carlsen, I. Misfeldt, and M. Mogensen, "Fission Product Behavior in High Burnup Reactor Fuel Subjected to Slow Power Increases," *Nucl. Tech.*, **72,** 258 (1986)
21. B.J. Lewis, "Fission Product Release from Nuclear Fuel by Recoil and Knockout," *J. Nucl. Mater.*, **148,** 28 (1987)
22. M.O. Tucker, "Grain Boundary Porosity and Gas Release in Irradiated UO_2," *Radiation Effects,* **53,** 251 (1980)
23. J.A. Turnbull and R.M. Cornell, "The Re-solution of Fission Gas Atoms from Bubbles During the Irradiation of UO_2 at an Elevated Temperature," *J. Nucl. Mater.*, **41,** 156 (1971)
24. Y.H. Koo, "The Computer Program FACTOR for Calculating the Radial Power Density and Burnup Factors in Fuel Pellets," Siemens Technical Report B412/90/E84 (1990)
25. R. Manzel, F. Sontheimer, and H. Stehle, "Fission Gas Release of PWR Fuel Under Steady and Transient Conditions Up to High Burnup," Light Water Reactor Fuel Performance, Orlando, Florida, April 21~24 (1985)
26. M.J.F. Notley, "A Computer Program to Predict the Performance of UO_2 Fuel Elements Irradiated at High Power Outputs to a Burnup of 10000 MWd/MTU," *Nucl. Appl. Technol.*, **9,** 195 (1970)
27. M. Oguma, "Cracking and Relocation Behavior of Nuclear Fuel Pellets During Rise to Power,"

Nucl. Eng. Des., **76,** 35 (1983)

28. R.G. Bellamy and J.B. Rich, "Grain Boundary Gas Release and Swelling in High Burnup Uranium Dioxide," *J. Nucl. Mater.*, **33,** 64 (1969)
29. C.E. Bayer, "An Evaluation of Published High Burnup Fission Gas Release Data," Light Water Reactor Extended Burnup-Fuel Performance and Utilization, Williamsburg, Virginia, April 4~8 (1982)
30. K.R. Merckx, "The Defomational Responses of Urania Fuel Pellets," *Res Mechanica*, **24,** 299 (1988)
31. G.E. Pile and C.H. Seager, "Percolation and Conductivity: A Computer Study I," *Phys. Rev. B*, **10,** 1421 (1974)